# Measurement of Vibration and Improving the Shaft Vibration Dynamics of Gear and Belt Drive Using a Vibration Analyzer

**Md. Sharful Insan[1], Mohammad Din Al Amin[2], Md. Emdadul Haque[1]**

[1]Dept. of Mechanical Engineering, Rajshahi University of Engineering and Technology,
[2]Dept. of Mechanical Engineering, Bangladesh University of Engineering and Technology

**Abstract**

Rotating elements are essential components in the industrial sector, where vibration is a common occurrence. Vibration has its bad impacts, which include damages, disturbances, noise, etc. As a result, every industry must quantify the effect of vibration and keep it below a certain threshold. To study the effect of vibration, a system is developed that consists of power transmitting elements such as a belt-pulley mechanism, spur gear, ball bearing, shaft, and a motor for power production. This rotating element's vibration is analyzed by a vibration analyzer, which contains three types of sensors that measure the vibration characteristics along three axes (X, Y, and Z) at a particular point and return the vibration characteristics in waveform and spectrum at different points. This article describes the vibration of the shaft during shaft misalignment, mechanical looseness, and mass unbalancing. During this condition, the vibration level at a specific point crosses the ISO standard. After shaft alignment, mass balancing, and using damper materials, these vibration levels reduce to a certain level lower than those of the previous conditions, which have been studied in this paper. The vibration analyzer evaluates these vibration levels to determine whether or not the machinery is in optimal condition. This study provides analysis and design engineers with practical guidance for considering noise and vibration in gear and belt drives.

**Keywords:** Stiffness; Vibration; Control; Amplitude

## Introduction

Vibration analysis is an extremely important technique for diagnosing mechanical vibrations in machines. It is based on the high information content of machine vibration signals, which serve as an indicator of machine condition and are used for fault diagnosis. Vibration analysis is fundamental in a predictive maintenance program, being widely used for the detection and monitoring of incipient and severe faults in machinery parts, like bearings, shafts, couplings, rotors, motors, etc.

Srinath and Das [1] were the first to analyze the vibration of a non-rotating, simply supported beam carrying a mass with rotary inertia placed at an arbitrary location on the span. Chivens and Nelson [2] investigated the influence of disk flexibility on the bending natural frequencies and critical speeds of an axisymmetric rotating shaft-disk system. Lee and Chun [3] developed the assumed modes method to investigate the effect of multiple flexible disks on the vibration modes of a flexible rotor of varying annular cross-section. Nelson and McVaugh [4] developed a finite element model to include the effects of rotary inertia, gyroscopic moments, and axial load of a rotor-bearing system with rigid disks. Qin and

Mao [5] developed a shaft element model adding torsional deformation for accurate estimation of the dynamic behavior of the coupled transverse-torsional motion that exists in large power systems Parker and Mote [7] solved the eigenvalue problem for a non-spinning coupled disk spindle-clamp vibration with the use of extended operator formulation. Later, Parker et al. extended that work to spinning asymmetric [8] and axisymmetric [9] disk-spindle systems.
All of these earlier studies [1-9] did not combine various vibration-producing devices (such as gears, rotating shafts, rotating masses, bearings, belt pulleys, and motors) in a single setup. However, every piece of this equipment is a part of the system we've constructed.
Vibration analysis is commonly used to identify issues such as imbalance, misalignment, bent shafts, faults in rolling bearings, eccentricity, resonance, sloppiness, rotor rub, fluid-film bearing instabilities, gear faults, and belt/sheave issues.
Vibration may influence the durability and reliability of mechanical systems or structures and cause problems such as damage, abnormal stopping, and disaster. Vibration analysis is one such tool, which is much preferred by people. It acts as a measurement tool and evaluates any failure in rotating machine equipment. Several technologies are used to measure and diagnose machine health. Two of the most important are vibration testing and infrared thermography. The use of a vibration analyzer is one of the simple, economical, and convenient methods to determine vibration level.

This project aims to realize the phenomenon of vibration and it also aims to design and construct the active vibratory system. Finally, a vibration analyzer is used for vibration measurement. In this paper vibration level of our developed system before misalignment of the shaft, mechanical looseness, and mass unbalancing, and after alignment of the shaft, mechanical fittings, and mass balancing are presented. On the basis of experimental data performance results are explored.

## VIBRATION ANALYZER

For model structure and vibration measurement, some elements are used i.e. vibration analyzer and sensors. The CSI 2140 is the most complete tool for assessing and predicting machinery health. The CSI 2140 builds on Emerson's industry-leading CSI 2130 to make route-based maintenance more efficient and predictive diagnostics more usable. Influenced by human-centered design principles and built with users in mind, the CSI 2140 meets both the usability and advanced diagnostics requirements of reliability engineers.


Fig 4.1: Front panel of CSI analyzer [10].

**set-up design**

With some notion of the arrangement of machine elements, we may begin the calculations. From data, such as the work done or power consumed, we compute forces on each part for a sequence of positions of the machine's cycle, using the principles of machines.

**Calculations of different parts of the set-up**

**A. Gear Indexing**

Indexing is an operation of dividing a periphery of a cylindrical workpiece into equal divisions with the help of an index crank and index plate.

**For plain indexing,**

the number of turns of the crank for each division, T = $\frac{40}{N}$ $\frac{40}{N}$ , Where N indicates the number of divisions required.

For driver gear (pinion) let, N = 60

Outside diameter, $D_o$ $D_o$ = 5 in

Number of turns for each division, T = $\frac{40}{N}$ $\frac{40}{N}$ $=\frac{40}{60}\frac{40}{60}=\frac{22}{33}$

So, the required number of turns for each division for pinion,

T = $\frac{2}{3}\times\frac{132}{133}\times\frac{13}{13}=\frac{2626}{3939}$

Therefore, for pinion it is decided to use plate-3 and for each division, crank should be turned for 26 holes of the 39-hole circle.

Again, for driven gear let, N = 44

Outside diameter, $D_o D_o$= 3 in

Number of turns for each division, T = $\frac{40}{N}$ $\frac{40}{N}$ $=\frac{40}{44}\frac{40}{44}=\frac{10}{11}\frac{10}{11}$

So, the required number of turns for each division for driven gear, T = $\frac{10}{11}\times\frac{310}{311}\times\frac{3}{3}=\frac{30}{33}\frac{30}{33}$

Therefore, for driven gear it is decided to use plate-2 and for each division crank should be turned for 30 holes of the 33-hole circle.

**B. Calculation of Gear Terminology**

Let, outside diameter of pinion, $D_o D_o$= 5

Diametral pitch, $P_d=\frac{N+2}{D_o}P_d=\frac{N+2}{D_o}=\frac{60+2}{5}\frac{60+2}{5}$ =12.4 ≈ 12

Clearance, C = $\frac{0.157}{P_d}\frac{0.157}{P_d}$ ≈ 0.013 in

Now, dedendum = addendum (A) + clearance (C)

= $\frac{1.157}{P_d}$ $\frac{1.157}{P_d}$ ≈ 0.096 in

Whole depth, $W_d$ $W_d$ = $\frac{2.157}{P_d}$ $\frac{2.157}{P_d}$ ≈ 0.179 in

Root diameter, $D_r D_r$= $D_o D_o$- (2×$W_d W_d$) = 4.64 in

Working depth = $W_d$ $W_d$ - C = 0.179 - 0.013 = 0.166 in

**C. Horse Power Calculation**

Let, teeth no of pinion,$N_p = 60$;$N_p = 60$; Face width, b= $1''$; = $1''$; diameter of pinion, $D_p = 5"$; $D_p = 5"$; revolution, $n_p n_p$=1150 rpm.

Speed, $V = \pi D_p n_p V = \pi D_p n_p = \pi \times \frac{5}{12} \times 1150 = \pi \times \frac{5}{12} \times 1150$=1505.35 fpm

$As\ V_m \leq\ 2000fpm,\ As\ V_m \leq\ 2000fpm,$ Commercially cut [11]

Dynamic load $F_d = \frac{600+V_m}{600} \times F_t F_d = \frac{600+V_m}{600} \times F_t$

$F_d = 3.51F_t$ $F_d = 3.51F_t$

Ultimate strength, $S_u = 20f$ $S_u = 20f$ (For ASTM 20);

$S_u = 20 + 20 \times \frac{40}{100}$ $S_u = 20 + 20 \times \frac{40}{100}$ = 28 ksi

Again, endurance strength $S_n = 0.4S_u S_n = 0.4S_u$=0.4x28 =11.2 ksi

But from the table, $S'_n = 10\ ksi, S'_n = 10\ ksi,$ which is more conservative.

Lewis form factor,$Y_p = 0.713\ [for\ 20^0\ full\ depth, load\ at\ middle] Y_p = 0.713\ [for\ 20^0\ full\ depth, load\ at\ middle]$

Strength reduction factor,

$K_f = 2\ [for\ load\ at\ midle K_f = 2\ [for\ load\ at\ midle\ ]$

$P_d = \frac{N_P}{D_p}$

=60/5=12

Again,

$F_S = \frac{SbY}{K_f P_d} F_S = \frac{SbY}{K_f P_d}$

$= \frac{10\times1000\times1\times0.713}{2\times12}$

= 297.08 lb.

Now,

$F_s = N_{SF} F_d$

Or, 297.08=2x$F_d$

Therefore,

$F_d$=148.54 lb.

Again,

$F_d$=3.51×$F_t$

$F_t$ = 42.32 lb.

Now, $hp = \frac{F_t \times V_m}{33000}$

$\frac{42.32\times1505.35}{33000} = \frac{42.32\times1505.35}{33000}$

= 1.93

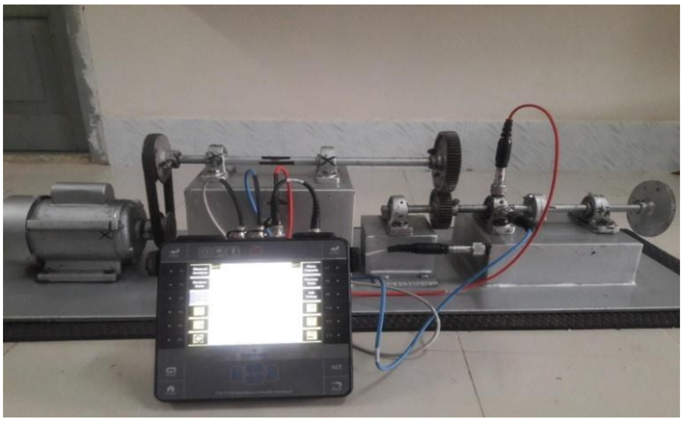

Fig.5: Experimental setup with vibration analyzer.

## Results

### *A.* Vibration Level Due To Shaft Misalignment And Mechanical Looseness

In the developed system there are two shafts that are connected parallel through spur gear. If the shafts are misaligned against each other, the vibration level will be increased. Mechanical looseness is also responsible for the increment of vibration. Non-rotating looseness causes the highest vibrations in the direction where the stiffness is the smallest. The stiffness is usually the least in the horizontal direction, but it depends on the physical layout of the machine. The loose foundation may be caused by loose bolts, nuts, or cracks. The following curves are found which were taken during the experiment.

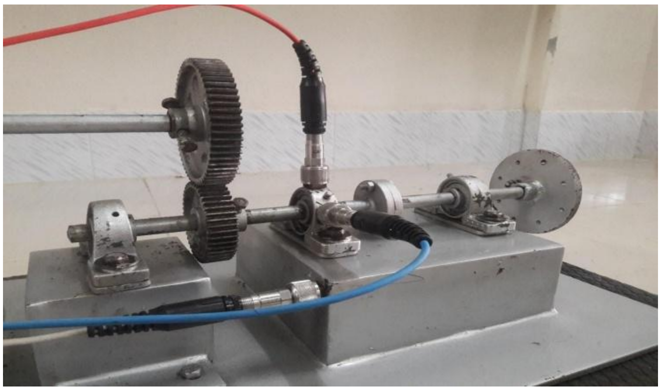

Fig 7.2: Vibration measurement at bearing 2.

**Spectrum plot with amplitude and frequency data at 2nd bearing**

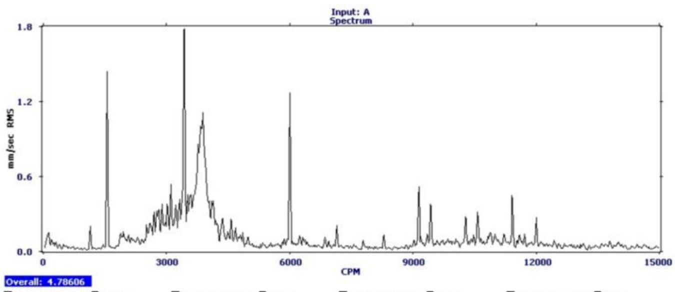


| Frequency Data | | Frequency Data | | Frequency Data | | Frequency Data | |
|---|---|---|---|---|---|---|---|
| 1555.3 | 1.43747 | 2803.7 | 0.38515 | 2881.6 | 0.40051 | 3008.0 | 0.42822 |
| 3108.2 | 0.55254 | 3218.3 | 0.40253 | 3311.4 | 0.46047 | 3421.9 | 2.08407 |
| 3500.3 | 0.48087 | 3572.0 | 0.52971 | 3777.0 | 0.97141 | 3834.1 | 1.16651 |
| 3873.5 | 1.23553 | 4022.3 | 0.46697 | 4095.8 | 0.45911 | 4116.6 | 0.45677 |
| 5998.5 | 1.26777 | 9124.3 | 0.56388 | 9421.4 | 0.43787 | 11408.2 | 0.50841 |

Acquired: 13/11/17 11:14 AM

Fig 7.3 : Vibration level of sensor A at bearing 2 (misalignment and mechanical looseness).

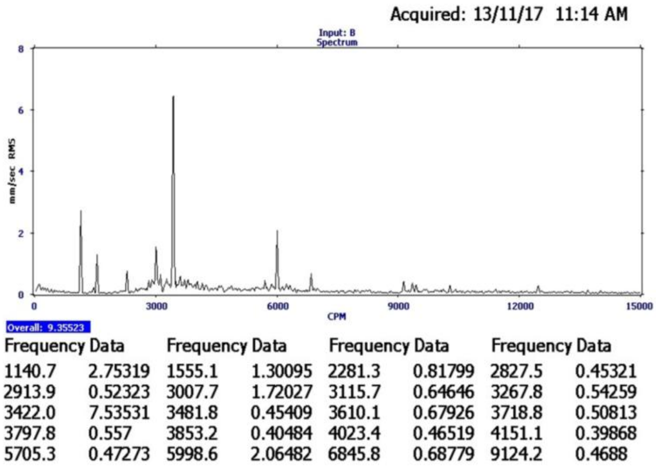


Fig 7.4: Vibration level of sensor B at bearing 2 (misalignment and mechanical looseness).

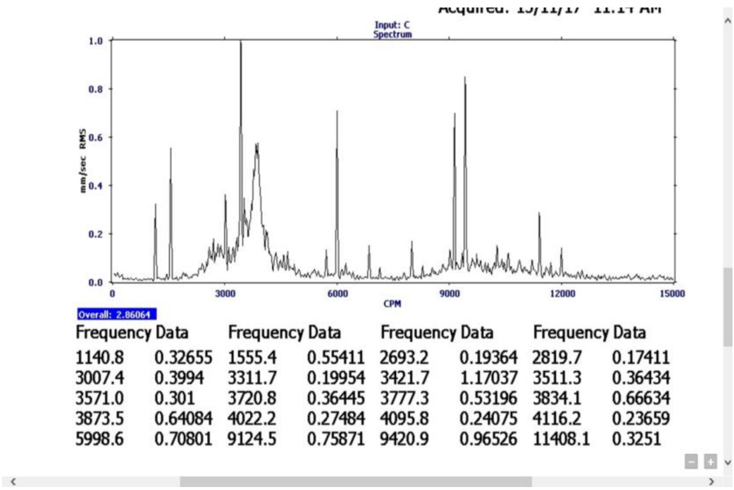


Fig 7.5: Vibration level of sensor C at bearing 2 (misalignment and mechanical looseness).

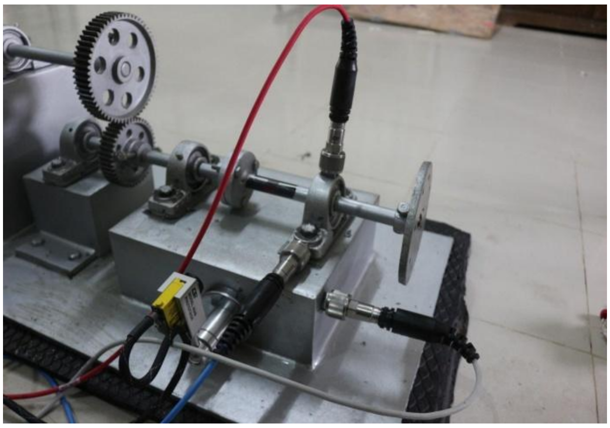

Fig 7.6: Vibration measurement at bearing 3.

**Spectrum plot with amplitude and frequency data at 3rd bearing**

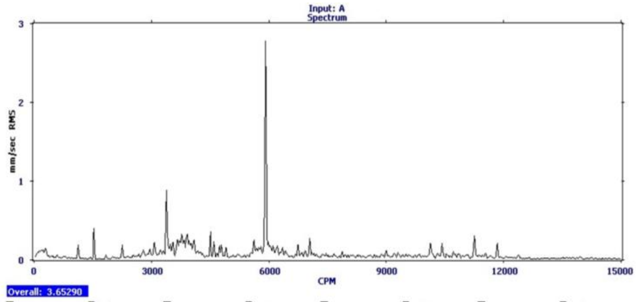


Overall: 3.65290

| Frequency | Data | Frequency | Data | Frequency | Data | Frequency | Data |
|---|---|---|---|---|---|---|---|
| 1532.1 | 0.41687 | 3066.5 | 0.25194 | 3371.2 | 0.90992 | 3553.0 | 0.2571 |
| 3665.2 | 0.29652 | 3721.7 | 0.27778 | 3776.6 | 0.3652 | 3835.6 | 0.28488 |
| 3909.9 | 0.37125 | 3949.4 | 0.25875 | 4004.6 | 0.23259 | 4078.5 | 0.2892 |
| 4495.2 | 0.3732 | 4598.5 | 0.24442 | 5617.4 | 0.27714 | 5912.0 | 2.93885 |
| 5973.7 | 0.24379 | 7036.9 | 0.28401 | 10114.7 | 0.23842 | 11236.8 | 0.31927 |

Acquired: 13/11/17 11:17 AM

Fig 7.7: Vibration level of sensor A at bearing 3 (misalignment and mechanical looseness).

Acquired: 13/11/17 11:17 AM

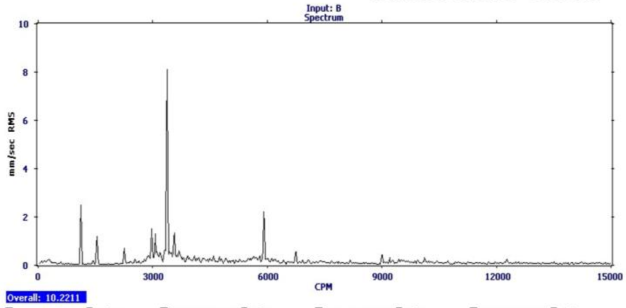


Overall: 10.2211

| Frequency | Data | Frequency | Data | Frequency | Data | Frequency | Data |
|---|---|---|---|---|---|---|---|
| 1123.7 | 2.49771 | 1532.2 | 1.23854 | 2247.6 | 0.71768 | 2878.7 | 0.45462 |
| 2963.1 | 1.49874 | 3064.2 | 1.4462 | 3104.4 | 0.6339 | 3195.5 | 0.58981 |
| 3327.0 | 0.71306 | 3371.0 | 8.3283 | 3439.1 | 0.62565 | 3479.4 | 0.60208 |
| 3554.9 | 1.47334 | 3625.0 | 0.45877 | 3681.4 | 0.63693 | 3911.4 | 0.42069 |
| 5787.0 | 0.42207 | 5912.3 | 2.34789 | 6741.5 | 0.62735 | 8989.7 | 0.49795 |

Fig 7.8: Vibration level of sensor B at bearing 3 (misalignment and mechanical looseness).

Acquired: 13/11/17 11:17 AM

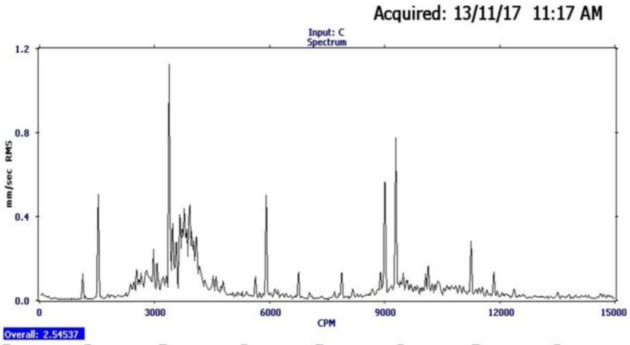


Overall: 2.54537

| Frequency | Data | Frequency | Data | Frequency | Data | Frequency | Data |
|---|---|---|---|---|---|---|---|
| 1532.0 | 0.53328 | 2959.8 | 0.24872 | 3066.1 | 0.20401 | 3371.1 | 1.15169 |
| 3461.5 | 0.40459 | 3553.5 | 0.32119 | 3664.5 | 0.46349 | 3721.8 | 0.39811 |
| 3776.5 | 0.4881 | 3835.9 | 0.37759 | 3909.9 | 0.52638 | 3963.1 | 0.35549 |
| 4005.2 | 0.31231 | 4077.8 | 0.35384 | 4152.8 | 0.19158 | 5912.0 | 0.53009 |
| 8990.6 | 0.66038 | 9283.5 | 0.78032 | 10116.3 | 0.18696 | 11236.7 | 0.29695 |

Fig 7.9: Vibration level of sensor C at bearing 3 (misalignment and mechanical looseness).

By analyzing the curves, it is evident that the indicated vibration level is not at the desired operating condition, i.e. it is surpassed the satisfied ISO limit. Due to this reason, to satisfy the ISO limit, we have to decrease the vibration limit.

<table>
<tr><th colspan="2">Velocity</th><th colspan="4">Velocity Range Limits and Machine Class</th></tr>
<tr><th>mm/s RMS</th><th>in/s Peak</th><th>Up to 15kW Class I</th><th>15 to 75kW II</th><th>>75 kW(Rigid) Class III</th><th>>75kW (Soft) Class IV</th></tr>
<tr><td>0.28</td><td>0.02</td><td rowspan="3">Good</td><td rowspan="4">Good</td><td rowspan="5">Good</td><td rowspan="6">Good</td></tr>
<tr><td>0.45</td><td>0.03</td></tr>
<tr><td>0.71</td><td>0.04</td></tr>
<tr><td>1.12</td><td>0.06</td><td rowspan="2">Satisfactory</td></tr>
<tr><td>1.80</td><td>0.10</td><td rowspan="2">Satisfactory</td></tr>
<tr><td>2.80</td><td>0.16</td><td rowspan="2">Unsatisfactory (Alert)</td><td rowspan="2">Satisfactory</td></tr>
<tr><td>4.50</td><td>0.25</td><td rowspan="2">Unsatisfactory (Alert)</td><td rowspan="2">Satisfactory</td></tr>
<tr><td>7.10</td><td>0.40</td><td rowspan="5">Unacceptable (Danger)</td><td rowspan="2">Unsatisfactory (Alert)</td></tr>
<tr><td>11.20</td><td>0.62</td><td rowspan="4">Unacceptable (Danger)</td><td rowspan="2">Unsatisfactory (Alert)</td></tr>
<tr><td>18.00</td><td>1.00</td><td rowspan="3">Unacceptable (Danger)</td></tr>
<tr><td>28.00</td><td>1.56</td><td rowspan="2">Unacceptable (Danger)</td></tr>
<tr><td>45.00</td><td>2.51</td></tr>
</table>

Fig 7.10: ISO limit of vibration level. The column named "Class I" in the above table is shown the operating condition of our 0.187 KW motor.

*B.* **Vibration Level After Tight Fittings Of The Bolts And Alignment Of The Shaft**

After shaft alignment and mechanical tight fittings of the bolts, the obtained values of vibration at bearing 2 and bearing 3 are comparatively lower than the shaft misalignment and mechanical looseness. The following curves which are found during the experiment show the decreased vibration levels at bearing 2 and 3. These decreased vibrations levels at that point are not satisfied with the ISO limit because of the lack of sufficient damper materials and unfixed of the setup base with the ground.

**Spectrum plot with amplitude and frequency data at 2nd bearing**

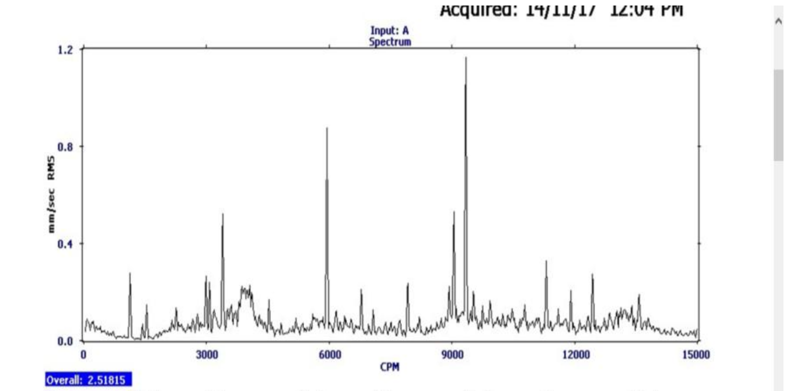


| Frequency Data | | Frequency Data | | Frequency Data | | Frequency Data | |
|---|---|---|---|---|---|---|---|
| 1129.1 | 0.2849 | 2974.5 | 0.28601 | 3080.3 | 0.25033 | 3387.4 | 0.55914 |
| 3854.6 | 0.25079 | 3928.2 | 0.25071 | 3984.2 | 0.24241 | 4042.5 | 0.25061 |
| 4095.8 | 0.22454 | 5944.2 | 0.87436 | 6775.4 | 0.22564 | 7904.2 | 0.26514 |
| 8918.9 | 0.23857 | 9031.3 | 0.56599 | 9331.2 | 1.25277 | 9514.2 | 0.2282 |
| 11290.4 | 0.33036 | 11885.7 | 0.20502 | 12420.1 | 0.30248 | 13549.1 | 0.21002 |

Fig 7.11: Vibration level of sensor A at bearing 2 (alignment and mechanical tight fittings).

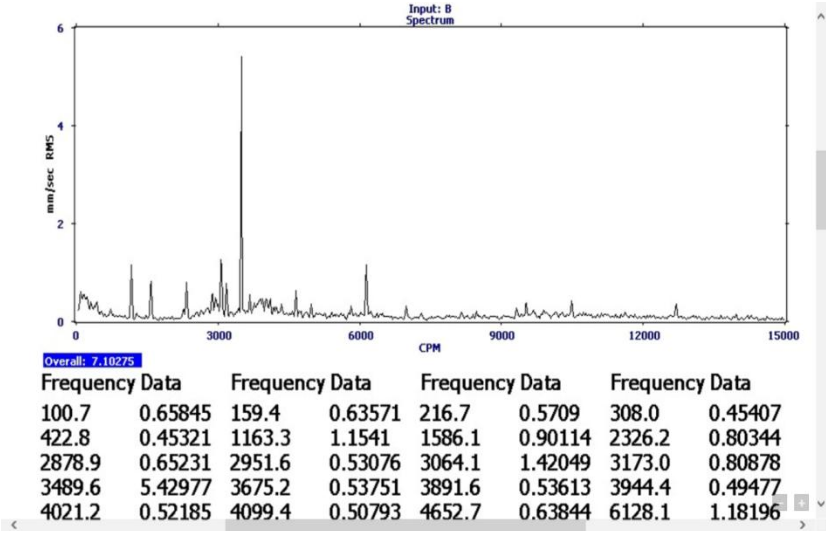


Fig 7.12: Vibration level of sensor B at bearing 2 (alignment and mechanical tight fittings).

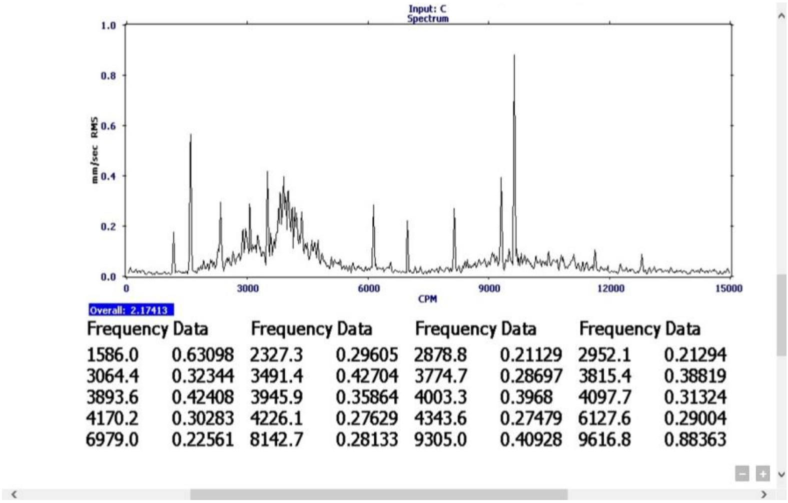


Fig 7.13: Vibration level of sensor C at bearing 2 (alignment and mechanical tight fittings).

**Spectrum plot with amplitude and frequency data at 3rd bearing**

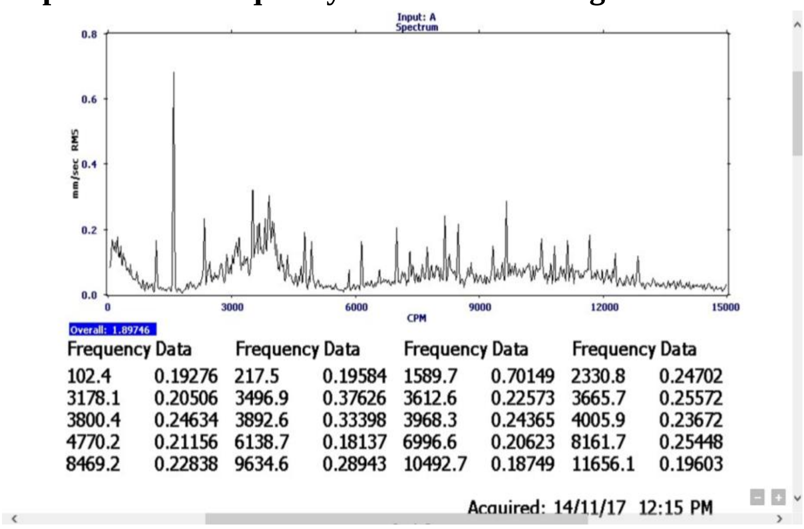


Fig 7.14: Vibration level of sensor A at bearing 3 (alignment and mechanical tight fittings).

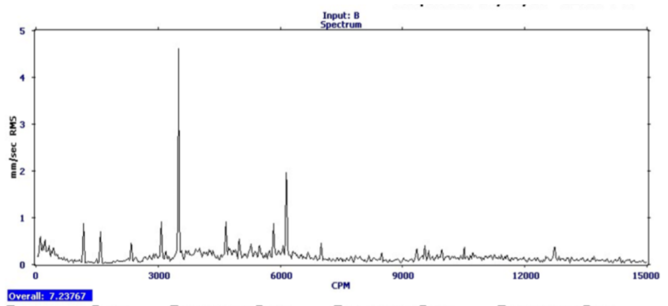


| Frequency | Data | Frequency | Data | Frequency | Data | Frequency | Data |
|---|---|---|---|---|---|---|---|
| 104.4 | 0.67708 | 173.8 | 0.44274 | 217.8 | 0.58312 | 313.7 | 0.43051 |
| 421.9 | 0.41328 | 1165.7 | 0.89464 | 1589.8 | 0.72015 | 2332.3 | 0.50971 |
| 3070.6 | 0.93487 | 3497.3 | 5.32604 | 4662.8 | 0.96991 | 4980.2 | 0.58996 |
| 5274.0 | 0.4641 | 5466.8 | 0.44674 | 5827.7 | 0.89824 | 6051.3 | 0.41356 |
| 6138.6 | 2.15684 | 6991.1 | 0.4568 | 9540.8 | 0.4136 | 12721.2 | 0.4326 |

Fig 7.15: Vibration level of sensor B at bearing 3 (alignment anb mechanical tight fittings).

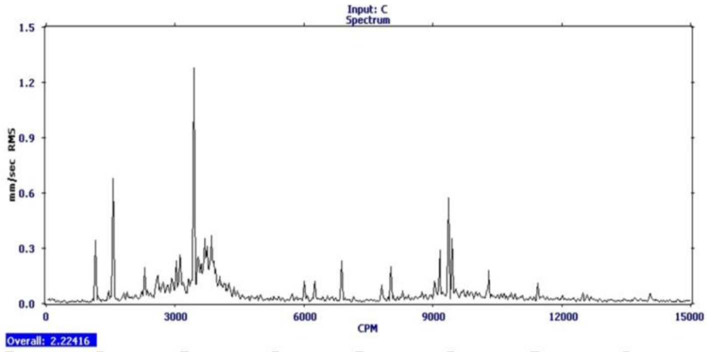


| Frequency | Data | Frequency | Data | Frequency | Data | Frequency | Data |
|---|---|---|---|---|---|---|---|
| 1143.3 | 0.33893 | 1559.6 | 0.6894 | 2286.3 | 0.19492 | 2597.8 | 0.17488 |
| 3014.0 | 0.23849 | 3120.5 | 0.29468 | 3430.3 | 1.2786 | 3516.8 | 0.28377 |
| 3591.4 | 0.24764 | 3689.1 | 0.36345 | 3743.0 | 0.33831 | 3847.3 | 0.37797 |
| 3891.0 | 0.26592 | 3930.0 | 0.20548 | 6860.2 | 0.23471 | 8003.6 | 0.20375 |
| 9145.5 | 0.29757 | 9354.1 | 0.57407 | 9435.8 | 0.36607 | 10288.9 | 0.18454 |

Fig 7.16: Vibration level of sensor C at bearing 3 (alignment and mechanical tight fittings).

## C. **Vibration Level Due To Mass Unbalancing**

Discordance between the mass axis and the rotation axis characterizes unbalance. The centrifugal force generated by rotation is the result of the unequal mass of the load and the radial acceleration caused by rotation. This causes a force on the bearings and/or bearing vibration. Because of the moment caused by the imbalance, the shaft vibrates in a way that is typical of rotating structures. Uniform circular cross-sections of the shafts are chosen, although the method developed is applicable to shafts with any cross-section having an axis of symmetry. The circular disk has a uniform thickness, with the center of mass coinciding with the axes of the corresponding shafts. Before mass unbalancing of the rotating load, vibration levels are shown below:

**Spectrum plot with amplitude and frequency data at 3rd bearing**

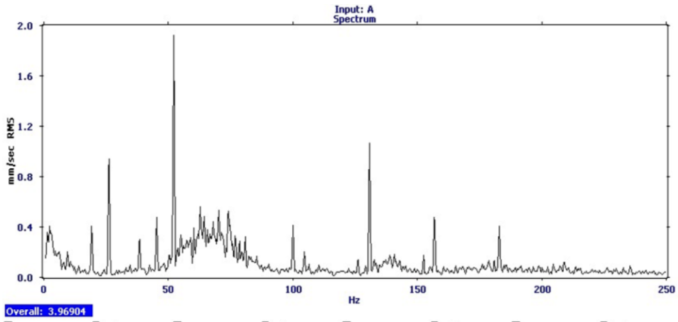


| Frequency | Data | Frequency | Data | Frequency | Data | Frequency | Data |
|---|---|---|---|---|---|---|---|
| 1.37 | 0.39458 | 2.31 | 0.44911 | 2.66 | 0.41256 | 19.15 | 0.42405 |
| 26.12 | 1.04785 | 45.27 | 0.48379 | 52.24 | 1.94832 | 60.14 | 0.44648 |
| 62.71 | 0.60004 | 64.26 | 0.52899 | 65.52 | 0.40367 | 67.71 | 0.47131 |
| 70.21 | 0.57162 | 71.39 | 0.40892 | 73.93 | 0.59455 | 74.53 | 0.47998 |
| 100.02 | 0.41688 | 130.58 | 1.07485 | 156.7 | 0.53779 | 182.78 | 0.40985 |

Acquired: 31/05/17 02:14 PM

Fig 7.17: Vibration level of sensor A at bearing 3 (mass unbalance).

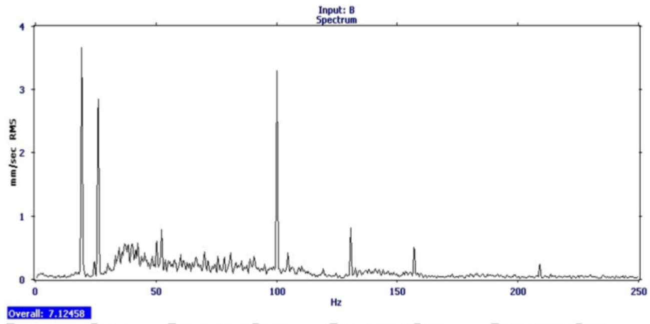


| Frequency | Data | Frequency | Data | Frequency | Data | Frequency | Data |
|---|---|---|---|---|---|---|---|
| 19.15 | 3.83838 | 26.12 | 3.19084 | 34.59 | 0.53812 | 35.81 | 0.48403 |
| 37.02 | 0.65008 | 38.28 | 0.63271 | 39.86 | 0.64788 | 41.4 | 0.54137 |
| 42.6 | 0.60811 | 45.41 | 0.43791 | 50.18 | 0.67283 | 52.25 | 0.80908 |
| 66.41 | 0.40987 | 69.89 | 0.47561 | 80.83 | 0.45126 | 90.45 | 0.41007 |
| 100.0 | 3.28775 | 104.47 | 0.44502 | 130.58 | 0.82685 | 156.71 | 0.57564 |

Fig 7.18: Vibration level of sensor B at bearing 3 (mass unbalance).

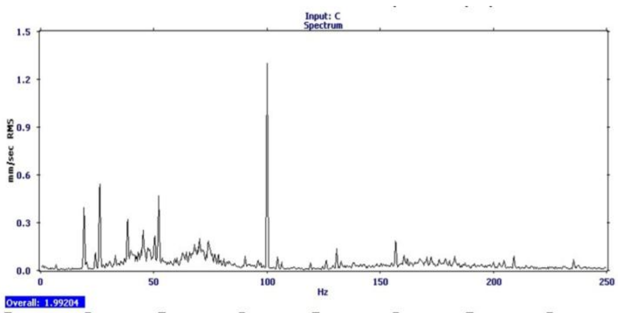


| Frequency | Data | Frequency | Data | Frequency | Data | Frequency | Data |
|---|---|---|---|---|---|---|---|
| 19.15 | 0.41304 | 26.11 | 0.61495 | 38.3 | 0.36251 | 39.82 | 0.14253 |
| 44.47 | 0.13346 | 45.22 | 0.26393 | 47.33 | 0.16253 | 47.98 | 0.14873 |
| 50.18 | 0.24427 | 52.24 | 0.47216 | 67.71 | 0.17103 | 68.28 | 0.14655 |
| 69.48 | 0.15669 | 70.21 | 0.21268 | 71.39 | 0.14871 | 71.72 | 0.14475 |
| 73.93 | 0.20527 | 100.0 | 1.29319 | 130.59 | 0.13781 | 156.7 | 0.20939 |

Fig 7.19: Vibration level of sensor C at bearing 3 (mass unbalance).

### *C.* Vibration Level After Mass Balancing

Using the trial and error method we gradually use an external different amount of masses at the different angles of the rotating load (impeller). Because the polar plot analysis identified the problem as a mass imbalance in the overhung impeller, a corrected mass was used to balance the rotor and reduce the intensity of vibration to a satisfactory level. The peak and phase data in Fig. 7.19 refer to the reason for such a high level of vibration. As a result, this value is primarily considered when considering the issue, and polar graph paper is used to reveal the unbalance issue.

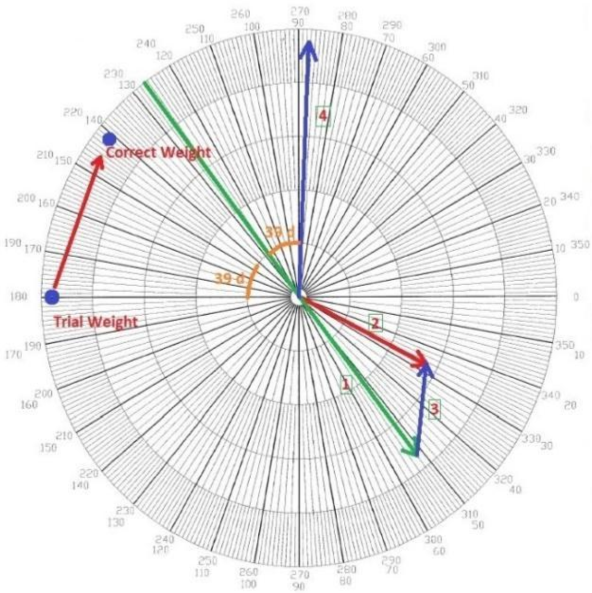


The correct weight is calculated using the following formula.

$$Correct\ weight = \frac{Length\ of\ vector\ 1 \times Trial\ weight}{Length\ of\ vector\ 3}$$

The length is measured with a fine scale ruler and the weight by a digital weighing scale. The measurements are as follows- The length of vector 1 was 6cm; the trial weight was 4.1gram; the length of vector 3 was 3 cm

So, the calculated correct weight required for balancing is,

$$Correct\ weight\ = \frac{6\ cm\ \times 3.1\ gm}{3\ cm} = 6.2\ gram$$

Table 1: Trial and error method for mass balancing

| Trial weight (gram) | Phase angle (degree) |
|---|---|
| (a). 3.5 | 270 |
| (b). 3.5 | 180 |
| (c). 4.3 | 225 |
| (d). 6.2 | 220 (desired angle) |

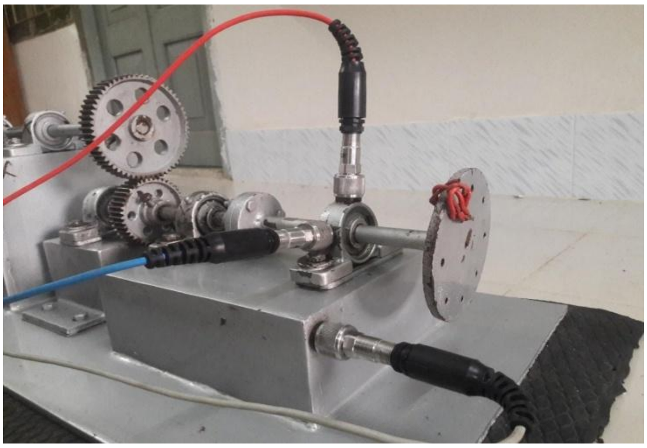

Fig 7.20: Balancing mass added in the rotating load.

After mass balancing the vibration level is reduced, spectrum plot with amplitude and frequency data at 3rd bearing is shown below:

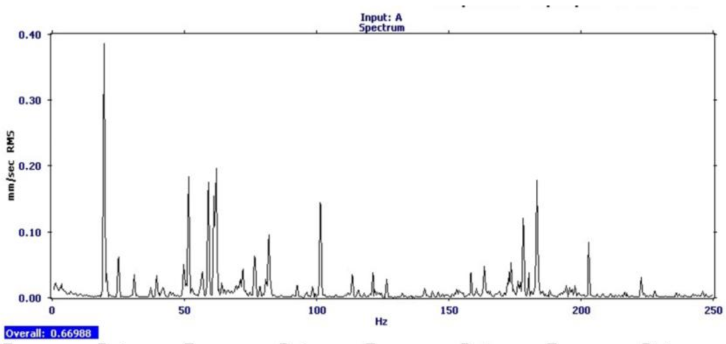


| Frequency Data | | Frequency Data | | Frequency Data | | Frequency Data | |
|---|---|---|---|---|---|---|---|
| 19.65 | 0.38834 | 24.87 | 0.0697 | 49.76 | 0.05266 | 51.48 | 0.19123 |
| 56.74 | 0.04351 | 58.94 | 0.19272 | 61.01 | 0.16002 | 61.78 | 0.20785 |
| 72.07 | 0.04793 | 76.39 | 0.07208 | 81.75 | 0.10485 | 101.4 | 0.16793 |
| 121.05 | 0.04096 | 158.29 | 0.04384 | 163.21 | 0.04925 | 172.55 | 0.03963 |
| 173.48 | 0.0531 | 177.93 | 0.13138 | 183.15 | 0.17852 | 202.79 | 0.08395 |

Fig 7.21: Vibration level of sensor A at bearing 3 (mass balance).

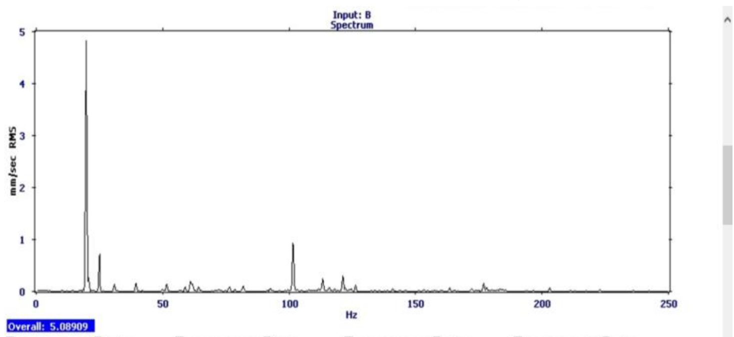


| Frequency Data | | Frequency Data | | Frequency Data | | Frequency Data | |
|---|---|---|---|---|---|---|---|
| 19.65 | 4.85442 | 20.54 | 0.27043 | 24.87 | 0.80091 | 30.89 | 0.14711 |
| 39.29 | 0.16556 | 51.48 | 0.15171 | 58.94 | 0.09779 | 61.06 | 0.21665 |
| 64.16 | 0.08805 | 76.44 | 0.09978 | 81.74 | 0.1144 | 101.4 | 1.06878 |
| 113.26 | 0.26849 | 115.8 | 0.07786 | 121.04 | 0.32614 | 122.01 | 0.07553 |
| 126.27 | 0.11699 | 163.39 | 0.06951 | 176.82 | 0.16104 | 177.92 | 0.08116 |

Fig 7.22: Vibration level of sensor A at bearing 3 (mass balance).

International Journal for Multidisciplinary Research (IJFMR)
E-ISSN: 2582-2160 ● Website: www.ijfmr.com ● Email: editor@ijfmr.com

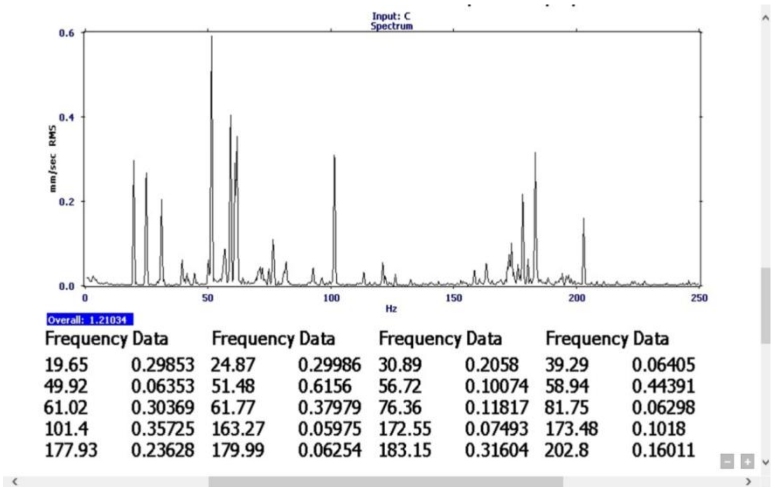


Fig 7.23: Vibration level of sensor C at bearing 3 (mass balance).

Table 2: Overall experimental data from graphs

| **Vibration measuring location** | **Conditions** | **Overall data of sensor A (mm/sec)** | **Overall data of sensor B (mm/sec)** | **Overall data of sensor C (mm/sec)** |
|---|---|---|---|---|
| Bearing 2 | Shaft misalignment & mechanical looseness | 4.78 | 9.36 | 2.86 |
| Bearing 2 | Shaft alignment & mechanical tight | 2.52 | 7.10 | 2.17 |
| Bearing 3 | Shaft misalignment & mechanical looseness | 3.65 | 10.22 | 2.54 |
| Bearing 3 | Shaft alignment & mechanical tight | 1.89 | 7.23 | 2.22 |
| Bearing 3 | Mass unbalancing | 3.97 | 7.12 | 2 |
| Bearing 3 | Mass balancing | 0.67 | 5.08 | 1.21 |

**Discussion & Conclusion**

A ball bearing having a regular bore was fabricated and was used for supporting the shaft at each end. This vibration-generating setup has been developed to measure vibration levels at different points by using a vibration analyzer. The vibration level of the experimental setup before and after shaft misalignment and mechanical looseness were investigated experimentally and compared with recorded data. From this, it can be concluded as follows:

- Mechanical looseness of the bolts, misalignment of the shaft, and mass unbalancing of the load-generated vibration. Which indicates the health condition of the machine.
- This vibration analyzer measures vibration level by using three types of sensors in spectrum and waveform. Where the measured vibration level is crossed the ISO limit. After alignment of the shaft, tightening the bolts mechanically, and mass balancing reduced the vibration level.
- Further reduction of vibration level, is also used damper materials under the base of the setup.
- The experimented vibration level at bearing 2 before shaft misalignment and mechanical looseness is 4.786 mm/sec, 9.355 mm/sec, and 2.86 mm/sec. After making the required changes the vibration levels are 2.52 mm/sec, 7.10 mm/sec, and 2.17 mm/sec respectively.
- Similarly, experimented results for bearing 3 before and after shaft misalignment and mechanical looseness are 3.65 mm/sec, 10.22 mm/sec, 2.55 mm/sec, and 1.89 mm/sec, 7.23 mm/sec, 2.22 mm/sec respectively.
- Mass balancing was also done on bearing 3 where the vibration before mass balancing is 3.97 mm/sec, 7.12 mm/sec, and 2 mm/sec. After mass balancing these vibrational values are 0.67 mm/sec, 5.08 mm/sec, and 1.21 mm/sec respectively.

**References**

1. L. S. Srinathand, Y. C. Das, "Vibrations of beams carrying mass". Transactions of the ASME, Journal of Applied Mechanics, vol. 34, pp. 784–785, 1967.
2. R. Chivens, and H. D. Nelson, "The natural frequencies and critical speeds of a rotating, flexible shaft-disk system". ASME Journal of Engineering for Industry, vol. 97, pp. 881–886, 1975.
3. C.-W. Lee, and S.-B. Chun, "Vibration analysis of a rotor with multiple flexible disks using assumed modes method". Journal of Vibration and Acoustics, vol. 120, pp. 87–94, 1998.
4. H. D. Nelson, and J. M. McVaugh, "The dynamics of rotor-bearing systems using finite elements". Journal of Engineering for Industry, vol. 98, May, pp. 593–600, 1976.
5. Q. H. Qin, and C. X. Mao, "Coupled torsional-flexural vibration of shaft systems in mechanical engineering-1 finite element model". Computers and Structures, vol. 58, no. 4, pp. 835–843, 1996.
6. S. S. Rao, "Mechanical Vibration" India: Dorling Kindersley, 2004.
7. R. G. Parker, and C. D. Mote, "Vibration and coupling phenomena in asymmetric disk-spindle system". ASME Journal of Applied Mechanics, vol. 63, pp. 953–961, 1996
8. R. G. Parker, "Analytical vibration of spinning, elastic disk-spindle systems". ASME Journal of Applied Mechanics, vol. 66, pp. 218–224, 1999.
9. P. J. Sathe, and R. G. Parker, "Free vibration and stability of a spinning disk spindle system". ASME Journal of Vibration and Acoustics, vol. 121, pp. 391–396, 1999.
10. http://www.emerson.com/documents/automation/CSI-2140-Machinery-Health-Analyzer-Quick-Start-Guide-en-39470.
11. Faires, "Design of machine elements" New York : The Macmillan company, 1962.